ACADEMIC PRESS

Available online at www.sciencedirect.com
SCIENCE DIRECT®

Journal of Catalysis 219 (2003) 97–106

JOURNAL OF CATALYSIS

www.elsevier.com/locate/jcat

Comparative study of *n*-pentane isomerization over solid acid catalysts, heteropolyacid, sulfated zirconia, and mordenite: dependence on hydrogen and platinum addition

N. Essayem,* Y. Ben Taârit, C. Feche, P.Y. Gayraud, G. Sapaly, and C. Naccache

Institut de Recherches sur la Catalyse, CNRS, conventionné UCB-Lyon, 2, Avenue Albert Einstein, 69626 Villeurbanne cedex, France

Received 18 October 2002; revised 27 January 2003; accepted 2 April 2003

Abstract

Skeletal isomerization of pentane over solid acid catalysts $(NH_4)_{2.5}H_{0.5}PW_{12}O_{40}$, sulfated zirconia, and H-mordenite has been studied. Hybrid bifunctional catalysts obtained by grinding equal weights of Pt/SiO_2 and each of the above solid acids were also used for the reaction. Various mechanistic aspects for *n*-pentane isomerization over monofunctional and bifunctional catalysts, in the presence or absence of hydrogen in the feed, are discussed. Analysis of product distributions at 423 and 473 K indicated that over monofunctional heteropolyacids and sulfated zirconia catalysts, the main reaction path is the bimolecular one, involving conjunct polymerization and cracking. Under these operating conditions the selectivity to isopentane is low. Monofunctional H-mordenite shows a significant activity only at 498 K. HPA and ZrO_2–SO_4, although showing stronger acidity than H-mordenite, do not activate *n*-pentane through a monomolecular path as "superacid-type catalysts" are expected to. Bifunctional isomerization of pentane appears at a reaction temperature of 473 K and up since the equilibrium concentration of pentene is significant only when the reaction temperature is 473 K and up. A monomolecular bifunctional mechanism is the preferred route for reaching high isomerization selectivity.

Keywords: Monomolecular; Bimolecular mechanism; Bifunctional catalyst; *n*-Pentane isomerization; Heteropolyacids; Sulfated zirconia; Mordenite; Effect of platinum; Effect of hydrogen

1. Introduction

The skeletal isomerization of C_5–C_6 paraffins is a key reaction in the petroleum industry, aimed at increasing the octane number of the gasoline pool. The reaction is equilibrium limited, low temperature favoring high thermodynamic concentrations of branched isomers. In order to achieve maximum isomer yields the isomerization of C_5–C_6 paraffins must be carried out at the lowest possible temperatures over highly efficient catalysts. Skeletal isomerization of alkanes is a typical acid-catalyzed reaction. Chlorinated alumina (Cl–Al_2O_3) containing platinum was found to be highly efficient for the isomerization of C_5–C_6 alkanes already at 423 K [1,2]. It is now well accepted that the reaction occurs through a monomolecular acid mechanism; the role of the platinum additive is to decrease the catalyst deactivation rate. It is also recognized that chlorinated alumina behaves like the so-called superacid, magic acid systems.

Zeolite-based catalysts have also been developed for the isomerization of C_5–C_6 [3–6]. Over H-mordenite-based catalysts, the reaction was carried out at a significantly higher temperature, 523 K. It was recognized that the acid strength of H-mordenite is less than that of Cl–Al_2O_3 which implies that a higher reaction temperature is required for the activation of C_5–C_6 alkanes. The efficiency of H-mordenite was improved by supporting platinum (or palladium) [3] and by dealumination [4]. More recently, other solid acid materials, exhibiting higher acid strength than that of H-mordenite, were applied to the skeletal isomerization of light alkanes. Among them the most efficient are heteropolyacid-based materials [7–10], sulfated zirconia [11–15], and tungstated zirconia (WO_x–ZrO_2) [16–18]. Promotion with platinum improves considerably the selectivity and stability with time on stream in the isomerization of light alkanes (C_4–C_6). For the isomerization of *n*-pentane over these heteropolyacids (HPA), sulfated zirconia (SO_4–

* Corresponding author.
E-mail address: nadine.essayem@catalyse.cnrs.fr (N. Essayem).

0021-9517/$ – see front matter
doi:10.1016/S0021-9517(03)00162-3

ZrO_2), tungstated zirconia (WO_x–ZrO_2), and platinum-free or platinum-containing catalysts, monomolecular and bimolecular mechanisms have been suggested. From the published results, it is clear that depending on the prevailing pathway, monomolecular versus bimolecular, and on the prevailing mechanism, monofunctional versus bifunctional, the presence of a dehydrogenating–hydrogenating component and the presence or absence of hydrogen will considerably affect the activity, selectivity, stability with time on stream, etc.

The aim of this work was to provide integrated experimental data on the skeletal isomerization of *n*-pentane over Pt-free and Pt-containing HPA, SO_4–ZrO_2, and H-mordenite catalysts where the effect of the reaction temperature and the effect of H_2 in the feed are investigated. Analysis of the degree of *n*-pentane conversion, the product distribution, and the stability with time on stream will allow further contributions to the understanding of the reaction mechanisms occurring under different reaction conditions.

2. Experimental

2.1. Catalysts

$(NH_4)_{2.5}PW_{12}O_{40}$ material was obtained by reacting $H_3PW_{12}O_{40}$ with an aqueous NH_4Cl solution containing the stoichiometric quantity of $NH_4{}^+$ ions to achieve the desired exchange level. The exchanged solid was then centrifuged and freeze dried. The specific surface area, measured by N_2 adsorption at 77 K, was 125 $m^2\,g^{-1}$. According to the model previously proposed [19] the material is described by layers of $H_3PW_{12}O_{40}$ (acid phase) supported on neutral $(NH_4)_3PW_{12}O_{40}$. The estimated proton density was 6.6×10^{17} $H^+\,m^{-2}$. This value was deduced from NH_3 adsorption at 373 K measured by gravimetry [19]. Fig. 1 shows the TGA and DTA curves recorded on $(NH_4)_{2.5}PW_{12}O_{40}$ salt up to 1023 K, under N_2 atmosphere, using a heating rate of 5 K min^{-1}. The decomposition of the ammonium salt starts at 833 K in agreement with previously published data [20]. For FTIR experiments, the ammonium salt was diluted in KBr (3 wt%).

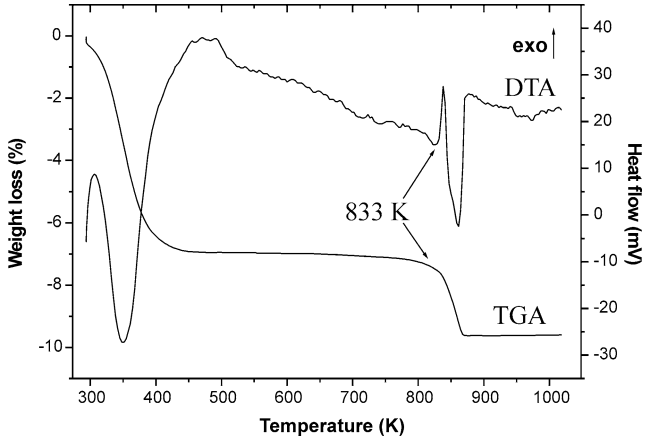

Fig. 1. TGA and DTA analyses of $(NH_4)_{2.5}H_{0.5}PW_{12}O_{40}$.

SO_4–ZrO_2 was obtained by reacting zirconium hydroxide with a 0.2 N H_2SO_4 solution [21]. The resulting solid was dried at 383 K, then calcined as the temperature was raised from 293 to 823 K, and maintained at this temperature for 2 h under dried air flow. Its BET surface area is equal to 100 $m^2\,g^{-1}$. The protonic density drawn from NH_3 adsorption at 373 K is equal to 22×10^{17} $H^+\,m^{-2}$. Prior to NH_3 adsorption the catalysts was heated in situ at 673 K under air for 2 h.

H-Mordenite was obtained by ion exchange of the Na form with a 1 N HCl solution. Hydrothermal treatment at 923 K followed by leaching with HCl solution at 293 K was applied to H-form mordenite. It resulted in a dealuminated H-mordenite with a framework $Si/Al = 10$. Calculated proton density is equal to 24×10^{17} $H^+\,m^{-2}$.

Pt/SiO_2 was prepared by impregnating SiO_2 support with a solution of chloroplatinic acid by the incipient wetness method to give a platinum content of 1%. The impregnated SiO_2 was dried at 373 K, calcined in air flow at 773 K and H_2 reduced at 673 K. Platinum dispersion measured by H_2 chemisorption was equal to 74%. In order to determine the optimal ratio in weight between Pt/SiO_2 and the acid material, an increased amount of Pt/SiO_2 was added to the acid material and the *n*-pentane conversion was measured at 473 K (or 498 K for H-mordenite) for each composition of the mixture. A stationary *n*-pentane conversion was found when equal amounts of Pt/SiO_2 and acid material are present in the hybrid catalyst. It followed that the *n*-pentane reaction was carried out over hybrid samples obtained by grinding together an equal weight of the acid solid with Pt/SiO_2 powder (Pt-containing catalyst) or with pure SiO_2 (Pt-free catalyst). To insure close contact between the two components a long grinding time was allowed (3 min).

2.2. Reaction of *n*-pentane

n-Pentane from Aldrich was used without further purification. It contains less than 0.5% isopentane impurity. The reaction of *n*-pentane is carried out in a continuous flow microreactor at atmospheric pressure, the reaction temperature was 423 or 473 K. Partial pressure of *n*-pentane was 14 Torr complemented to atmospheric pressure either by N_2 or by H_2. Total flow rate was 1.3 L h^{-1}. The amount of 0.6 g of the mixed catalysts was used, the sample in the reactor containing always 0.3 g of the acid component. Prior to the reaction, the catalyst was treated in situ at 673 K in air for 2 h and then at 473 K in H_2 for 2 h as well as for the zeolitic material than for the sulfated zirconia sample. For the HPA-based catalyst, only an in situ reduction in H_2 at 473 K for 2 h was applied prior the catalytic test. *n*-Pentane and reaction products were analyzed by on-line gas chromatography equipped with a flame ionization detector and a CP-Sil2CB fused silica capillary column.

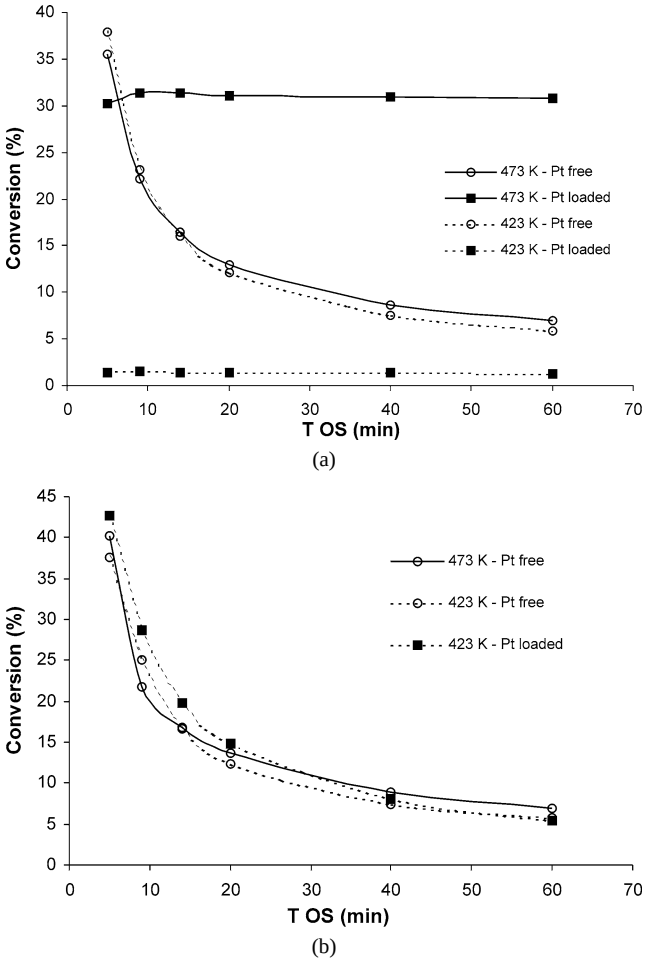

Fig. 2. *n*-Pentane reaction over $(NH_4)_{2.5}H_{0.5}PW_{12}O_{40}$-based catalysts (a) *in* H_2 and (b) *in* N_2. Reaction conditions: *n*-pentane pressure was 14 Torr diluted *in* H_2 (a) and N_2 (b) to atmospheric pressure. Total flow rate = 1.3 L h^{-1}. *m* Catalysts: Pt free, 0.3 g $(NH_4)_{2.5}H_{0.5}PW_{12}O_{40}$ + 0.3 g SiO_2; Pt loaded, 0.3 g $(NH_4)_{2.5}H_{0.5}PW_{12}O_{40}$ + 0.3 g Pt/SiO_2. Catalysts pretreatment: 2 h at 473 K under H_2 or N_2 flow for Pt-loaded or Pt-free material, respectively.

3. Results

3.1. $(NH_4)_{2.5}H_{0.5}PW_{12}O_{40}$ catalysts

The conversion of *n*-pentane with time on stream over HPA-based catalysts is shown in Figs. 2a and 2b, respectively in the presence or absence of H_2 in the feed. Over Pt-containing $(NH_4)_{2.5}H_{0.5}PW_{12}O_{40}$, the presence of H_2 in the feed had an inhibiting effect on the conversion at 423 K, the reaction of *n*-C_5 being almost suppressed (Fig. 2a), and a stabilizing effect at 473 K as indicated by the absence of significant catalyst deactivation with time on stream (Fig. 2a). The positive effect of H_2 on the catalyst stability with TOS occurred only at the higher reaction temperature (473 K) and in the presence of platinum. Indeed Figs. 2a and 2b show that over Pt-free acidic ammonium salt, even at 473 K, the conversion of *n*-C_5 decreased strongly with time on stream irrespective of the presence of H_2. Fig. 2b shows also that at

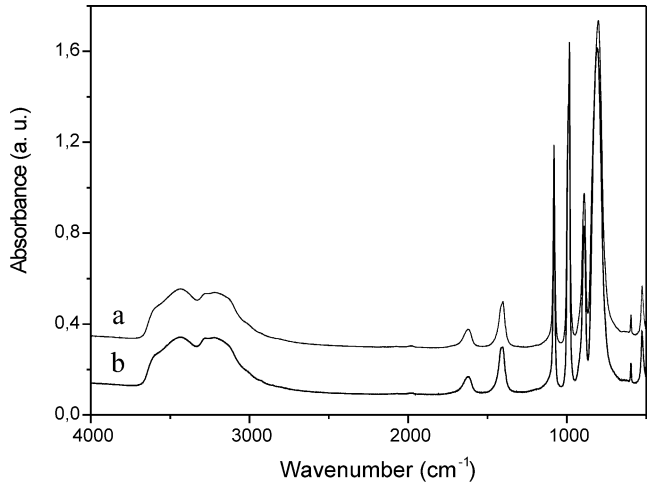

Fig. 3. IR spectra of fresh and used $(NH_4)_{2.5}H_{0.5}PW_{12}O_{40}$ catalysts. (a) Fresh $(NH_4)_{2.5}PW_{12}O_{40}$; (b) used $(NH_4)_{2.5}PW_{12}O_{40}$. Reaction conditions: 14 Torr *n*-C_5 diluted in H_2, $T_R = 473$ K. Total flow rate = 1.3 L h^{-1}; *m* catalyst, 0.3 g $(NH_4)_{2.5}H_{0.5}PW_{12}O_{40}$.

423 K, Pt-containing HPA, in the absence of H_2, showed a significant initial activity but deactivated with time on stream. The IR spectra of the fresh and used ammonium salt (Pt-free HPA) are presented in Fig. 3. The used catalyst is that recovered after the experiment performed under hydrogen at the highest temperature, 473 K. One can observe that the vibrations due to the Keggin unit (700–1100 cm^{-1}) and the intensity of the NH_4^+ band at 1410 cm^{-1} remained almost unchanged. These data indicate that the deactivation observed with the time on stream was not caused by a structural modification of the heteropolyacid.

The apparent absence of a temperature effect on the conversion level over Pt-free catalyst, in H_2 or in N_2, must be considered as an artifact due to the strong initial deactivation. Apparently, as might be anticipated, the rate of deactivation was higher at 473 K than at 423 K resulting in a higher impact on the conversion at 473 K.

To summarize, it is important to underline two important results:

- The simultaneous presence of hydrogen and platinum inhibits and even suppresses the reaction of *n*-C_5 at 423 K over HPA-based catalysts.
- The presence of H_2 by itself without added platinum to HPA cannot improve the catalytic stability with time on stream at 423 and 473 K.

The peculiar catalytic behavior of Pt-free and Pt-containing HPA catalysts with the reaction temperature and with the presence of H_2 in the feed was also reflected on the reaction product distribution. Tables 1 and 2 list the product distribution with time on stream for *n*-pentane reaction over Pt-free and Pt-containing HPA catalysts. These tables show also the respective effects of the reaction temperature and of the presence of H_2 in the feed. *Over Pt-free HPA* the reaction of *n*-C_5 at 423 and 473 K in the absence or presence

Table 1
n-Pentane reaction over $(NH_4)_{2.5}H_{0.5}PW_{12}O_{40}$-based catalysts *in* H_2: product distribution

	Pt loaded						Pt free					
T_R (K)	423			473			423			473		
TOS (min)	5	20	60	5	20	60	5	20	60	5	20	60
Conversion (%)	1.1	1.4	1.3	30.0	31.0	31.0	38.0	12.0	5.8	36.0	13.0	6.9
C_1–C_3	–	–	–	–	–	–	5.5	3.3	2.3	7.6	4.0	2.7
iC_4	–	–	–	0.1	0.1	0.1	57.0	37.0	26.0	48.0	29.0	21.0
n-C_4	–	–	–	–	–	–	4.0	1.9	0.3	5.0	2.1	1.6
iC_5	100.0	100.0	100.0	99.9	99.8	99.8	29.0	50.0	63.0	34.0	57.0	67.0
C_6	–	–	–	–	0.1	0.1	4.1	7.7	8.1	5.3	7.8	7.9

Reaction conditions: *n*-pentane pressure was 14 Torr diluted *in* H_2 to atmospheric pressure. Total flow rate = 1.3 L h^{-1}. *m* Catalysts: Pt free, 0.3 g $(NH_4)_{2.5}H_{0.5}PW_{12}O_{40}$ + 0.3 g SiO_2; Pt loaded, 0.3 g $(NH_4)_{2.5}H_{0.5}PW_{12}O_{40}$ + 0.3 g Pt/SiO_2. Catalysts pretreatment: 2 h at 473 K under H_2 flow or N_2 flow for Pt-loaded or Pt-free, respectively.

Table 2
n-Pentane reaction over $(NH_4)_{2.5}H_{0.5}PW_{12}O_{40}$-based catalysts *in* N_2: product distribution

	Pt loaded			Pt free					
T_R (K)	423			423			473		
TOS (min)	5	20	60	5	20	60	5	20	60
Conversion (%)	43.0	15.0	5.5	38.0	12.0	6.0	40.0	14.0	6.9
C_1–C_3	6.5	2.5	1.1	5.3	3.3	2.2	7.5	3.9	2.6
iC_4	62.0	53.0	38.0	57.2	39.0	26.0	48.0	28.0	20.0
n-C_4	6.2	3.9	2.6	4.5	0.6	0.3	5.0	2.2	1.5
iC_5	22.0	35.0	51.0	29.0	49.0	61.0	34.0	58.0	68.0
C_6	2.8	5.2	6.9	4.0	7.6	8.1	5.5	7.8	7.6

Reaction conditions: *n*-pentane pressure was 14 Torr diluted *in* N_2 to atmospheric pressure. Total flow rate = 1.3 L h^{-1}. *m* Catalysts: Pt free, 0.3 g $(NH_4)_{2.5}H_{0.5}PW_{12}O_{40}$ + 0.3 g SiO_2; Pt loaded, 0.3 g $(NH_4)_{2.5}H_{0.5}PW_{12}O_{40}$ + 0.3 g Pt/SiO_2. Catalysts pretreatment: 2 h at 473 K under H_2 or N_2 flow for Pt-loaded or Pt-free material, respectively.

of H_2 resulted in the formation of small quantities of C_1–C_3 and C_6 alkanes; isobutane and isopentane were the main products. At the initial reaction time the production of isobutane exceeded largely the production of isopentane. It is also interesting to point out that the selectivity toward isopentane with respect to isobutane increased with the reaction temperature and also increased with time on stream. The reaction of *n*-pentane at 423 K in the absence of H_2 *over Pt-containing HPA* also produced mainly isobutane and isopentane, again the isobutane concentration exceeding isopentane at the initial reaction time (Table 2). However, in H_2, although the n-C_5 conversion at 423 K was very low, 1%, the only product formed was isopentane. At 473 K, in H_2, the conversion of n-C_5 was substantial and the product formed was essentially isopentane (Table 1). The qualitative differences between the reaction of *n*-pentane over Pt-free and Pt-containing HPA when H_2 was present in the feed indicate that the mechanisms of the reaction of *n*-pentane differ considerably with the experimental conditions.

3.2. Sulfated zirconia (SO_4–ZrO_2) catalysts

Figs. 4a and 4b show the conversion of *n*-pentane versus time on stream respectively in H_2 or in N_2, over Pt-free and Pt-containing sulfated zirconia catalysts. As shown in Figs. 4a and 4b the conversion of n-C_5 over *Pt-free samples* decreased rapidly with time on stream. The fast deactivation of the catalyst apparently occurred whatever the reaction temperature (423 or 473 K) and also similarly with or without added H_2. The behavior *of Pt-containing SO_4–ZrO_2* was comparable to that of Pt-containing HPA. At low reaction temperature, 423 K, and in the presence of H_2, no conversion of pentane was observed (Fig. 4a). At higher temperature 473 K, in the presence of H_2, a significant conversion of n-C_5 was observed and furthermore the catalyst did not deactivate with time on stream. In the absence of H_2 the conversion of n-C_5 at 473 K was higher than that in H_2, but fast deactivation with time on stream occurred (Fig. 4a). It is clear that for this catalyst H_2 had a negative effect on the initial conversion of *n*-pentane.

Tables 3 and 4 list the product selectivities for the reaction of n-C_5 respectively with or without H_2 in the feed. Results from these tables show that *Pt-free SO_4–ZrO_2* produced the same product distribution at 423 K irrespective of the presence of H_2 in the feed, isobutane being predominantly formed. Isobutane and isopentane were the major products observed. Small quantities of C_1–C_3 and C_6 were observed. The presence of a platinum component on *the hybrid Pt/SiO_2–SO_4–ZrO_2* catalyst produced a drastic effect on its catalytic performances. Although this catalyst behaved similarly as previously when the n-C_5 reaction was carried out at 473 K in the absence of H_2, when H_2 was present in the feed the rate of the reaction at 423 K was dramat-

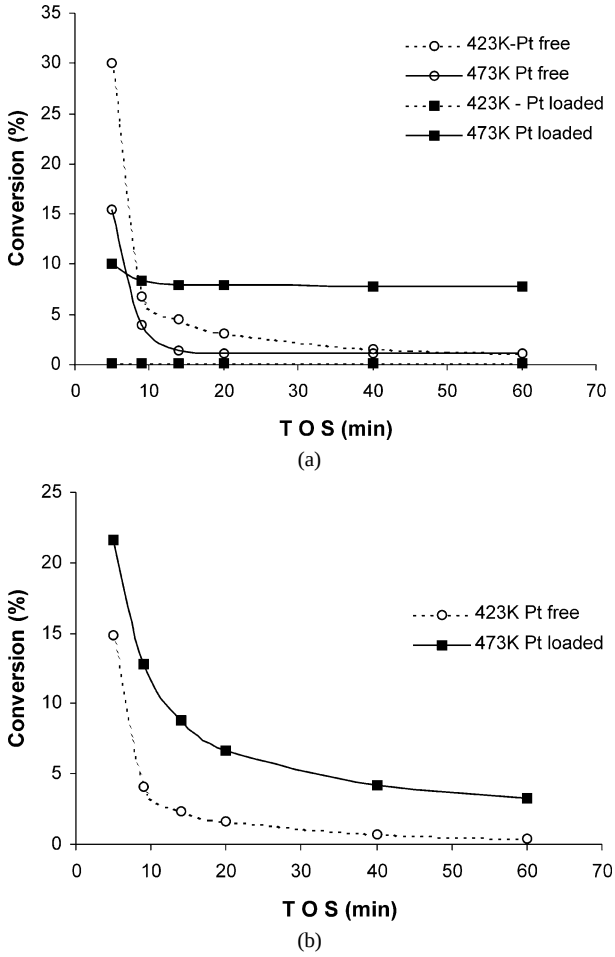

Fig. 4. n-Pentane reaction over SO_4–ZrO_2-based catalysts (a) *in* H_2 and (b) *in* N_2. Reaction conditions: n-pentane pressure was 14 Torr diluted *in* H_2 (a) and N_2 (b) to atmospheric pressure. Total flow rate = 1.3 L h^{-1}. *m* Catalysts: Pt free, 0.3 g SO_4–ZrO_2 + 0.3 g SiO_2; Pt loaded, 0.3 g SO_4–ZrO_2 + 0.3 g Pt/SiO_2. Catalysts pretreatment: Pt free, 2 h at 673 K under air flow; Pt loaded, 2 h at 673 K under air flow and then 2 h at 473 K in H_2 flow.

ically affected, the activity of sulfated zirconia being near zero. However, when the reaction temperature was raised to 473 K, conversion of n-pentane in the presence of H_2 occurred, selectivity toward isopentane was high. Only trace amounts of isobutane and 1-hexane were detected. These results indicate that sulfated zirconia exhibited a catalytic behavior in the reaction of n-pentane similar to that of heteropolyacid materials.

Table 4
n-Pentane reaction over SO_4–ZrO_2-based catalysts *in* N_2: product distribution

	Pt loaded			Pt free		
T_R (K)	473			423		
TOS (min)	5	20	60	5	20	60
Conversion (%)	21.6	6.7	3.3	15.0	1.6	0.4
C_1–C_3	8.1	4.1	2.7	8.2	6.9	6.3
iC_4	43.1	27.6	21.8	61.7	53.0	49.6
n-C_4	9.2	7.2	5.1	1.7	0.8	–
iC_5	33.0	49.0	60.3	23.8	29.5	27.8
C_6	6.7	12.1	10.0	4.6	9.7	16.3

Reaction conditions: n-pentane pressure was 14 Torr diluted *in* N_2 to atmospheric pressure. Total flow rate = 1.3 L h^{-1}. *m* Catalysts: Pt free, 0.3 g SO_4–ZrO_2 + 0.3 g SiO_2; Pt loaded, 0.3 g SO_4–ZrO_2 + 0.3 g Pt/SiO_2. Catalysts pretreatment: Pt free, 2 h at 673 K under air flow; Pt loaded, 2 h at 673 K under air flow and then 2 h at 473 K in H_2 flow.

3.3. H-Mordenite catalysts

At 423 K, neither bare H-M nor hybrid Pt/SiO_2-HM showed a detectable n-pentane reaction or in the presence or absence of H_2 in the feed. These observations are in good agreement with previously published results indicating that somewhat higher temperatures must be employed. The reaction was thus performed at 498 K. The n-C_5 conversion in H_2 or in N_2 over bare H-M and hybrid Pt/SiO_2-HM is shown in Figs. 5a and 5b. Clearly Fig. 5 shows that *bare H-M* has a significant activity for the reaction of n-pentane. The presence of H_2 in the feed has no significant effect on the conversion level or on the deactivation rate. *On hybrid* Pt/SiO_2*-HM* catalysts, H_2 in the feed exerted a profound effect on both the conversion level and the stability with time on stream. Fig. 5a shows that H_2 depressed the rate of n-C_5 conversion but simultaneously increased the stability with TOS. Table 5 summarizes the results, conversions, and product distribution, for the reaction of n-pentane at 498 K over

Table 3
n-Pentane reaction over SO_4–ZrO_2-based catalysts *in* H_2: product distribution

	Pt loaded						Pt free					
T_R (K)	423			473			423			473		
TOS (min)	5	20	60	5	20	60	5	20	60	5	20	60
Conversion (%)	0.2	0.1	–	10.0	8.0	7.8	30.0	3.1	1.1	15.4	1.2	1.1
C_1–C_3	–	–	–	0.6	0.5	0.5	9.1	6.6	6.0	8.2	2.4	2.2
iC_4	–	–	–	0.6	0.4	0.4	59.7	49.9	47.3	38.5	7.6	7.0
n-C_4	–	–	–	0.1	–	–	5.5	0.7	–	4.8	0.8	0.8
iC_5	100.0	100.0	–	97.7	98.3	98.5	21.6	34.1	34.6	41.7	82.4	83.1
C_6	–	–	–	1.0	0.7	0.6	4.1	8.6	12.1	6.8	6.8	6.8

Reaction conditions: n-pentane pressure was 14 Torr diluted *in* H_2 to atmospheric pressure. Total flow rate = 1.3 L h^{-1}. *m* Catalysts: Pt free, 0.3 g SO_4–ZrO_2 + 0.3 g SiO_2; Pt loaded, 0.3 g SO_4–ZrO_2 + 0.3 g Pt/SiO_2. Catalysts pretreatment: Pt free, 2 h at 673 K under air flow; Pt loaded, 2 h at 673 K under air flow and then 2 h at 473 K in H_2 flow.

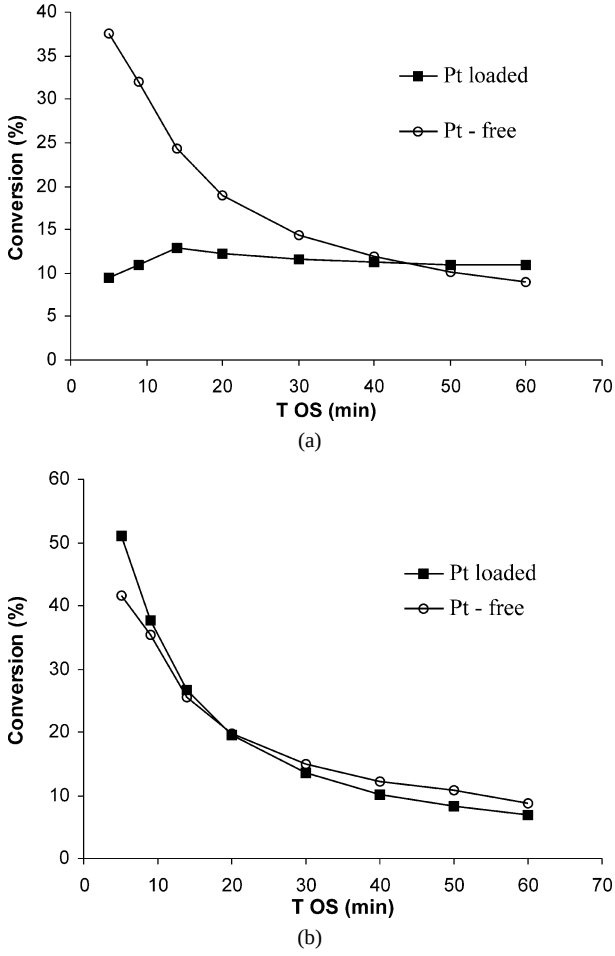

Fig. 5. *n*-Pentane reaction over H-mordenite-based catalysts at 498 K (a) *in H_2* and (b) *in N_2*. Reaction conditions: *n*-pentane pressure was 14 Torr diluted *in H_2* (a) and N_2 (b) to atmospheric pressure. Total flow rate = 1.3 L h^{-1}. *m* Catalysts: Pt free, 0.3 g H-mordenite + 0.3 g SiO_2; Pt loaded, 0.3 g H-mordenite + 0.3 g Pt/SiO_2. Catalysts pretreatment: Pt free, 2 h at 673 K under air flow; Pt loaded, 2 h at 673 K under air flow and then 2 h at 473 K in H_2 flow.

bare and hybrid H-mordenite catalysts. The effects of the presence of H_2 in the feed are also given. Over *bare H-M* in the absence or presence of H_2, C_4 paraffins (isobutane and butane) were predominantly formed. At the initial reaction time the C_4 fraction represents more than 60% of the products. It is also interesting to note that isopentane selectivity was less than 20%. *Hybrid Pt/SiO_2-HM* catalysts produced similar catalytic properties, conversion and product distribution, and stability with time on stream, when the reaction of *n*-pentane was performed in the absence of H_2. The addition of H_2 in the feed not only suppressed the deactivation with time on stream but also depressed the level of conversion observed in the absence of H_2 and more importantly increased drastically the selectivity to isopentane up to 84%. Only small amounts of C_4 alkanes were observed (around 8%).

4. Discussion

The acid strength of $H_3PW_{12}O_{40}$ was found to be higher than that of zeolites like H-ZSM-5 and H-mordenite [22,23]. Although the term of "superacid" for these materials HPA and SO_4–ZrO_2 has been disputed, it is well agreed that their acid strength is higher than that of zeolites. The results on pentane isomerization confirm this ranking of the superior acid strength of HPA and SO_4–ZrO_2 compared to H-mordenite [23]. Bare HPA and SO_4–ZrO_2, over which the *n*-pentane reaction is catalyzed by a monofunctional acid reaction, are active for *n*-pentane already at 423 K, similarly to chlorinated alumina. These findings imply that under the present conditions of temperature, pressure, and molar hydrogen to pentane ratio, HPA and SO_4–ZrO_2 activate pentane while H-mordenite cannot. The lack of *n*-pentane reaction at 423 K over H-mordenite reflects how difficult the activation of lower alkanes is and how weak the acid sites of H-mordenite are. In a previous work [24] it was indicated that Pt/H-mordenite was as active as Pt/SO_4–ZrO_2 for the isomerization of *n*-pentane. Although not clearly understood, the discrepancy may be due to differences in catalyst compositions and reaction conditions employed in [24] and in this work. Nevertheless our results clearly and unambiguously demonstrate that bare H-mordenite is much less efficient than HPA and SO_4–ZrO_2 for the isomerization of *n*-pentane.

Table 5
n-Pentane reaction over H-M and Pt–SiO_2/H-M at 498 K: product distribution

	H-M						Pt–SiO_2/H-M					
	in N_2			in H_2			in N_2			in H_2		
TOS (min)	5	20	60	5	20	60	5	20	60	5	20	60
Conversion (%)	41.6	19.8	8.8	32.0	18.9	9.0	50.6	19.6	6.8	10.9	12.3	10.9
C_1–C_3	19.3	20.4	21.0	19.9	19.5	19.3	19.5	20.1	21.5	7.1	9.5	6.1
iC_4	47.1	33.8	25.6	40.2	32.4	24.0	41.3	27.8	19.6	3.7	3.2	2.0
n-C_4	16.6	17.1	19.2	18.5	17.7	18.7	13.5	14.9	15.6	4.2	8.3	5.7
iC_5	15.7	24.1	28.5	18.2	25.3	31.7	22.5	31.4	37.3	84.1	77.5	84.9
C_6	1.6	4.5	5.7	3.2	5.0	6.3	3.2	5.8	6.0	0.9	1.7	1.3

Reaction conditions: *n*-pentane pressure was 14 Torr diluted in N_2 or in H_2 to atmospheric pressure. Total flow rate = 1.3 L h^{-1}. *m* Catalysts: Pt free, 0.3 g H-mordenite + 0.3 g SiO_2; Pt loaded, 0.3 g H-mordenite + 0.3 g Pt/SiO_2. Catalysts pretreatment: Pt free, 2 h at 673 K under air flow; Pt loaded, 2 h at 673 K under air flow and then 2 h at 473 K in H_2 flow.

Monomolecular or/and bimolecular mechanisms have been proposed for the isomerization of *n*-pentane over strong solid acids such as sulfated zirconia [10,13,14,25] and Pt/WO_x–ZrO_2 [18]. Conclusions have been drawn on the bases of the product distribution monitored by ^1H and ^{13}C NMR, obtained in the presence of Pt and in the presence of CO or H_2 in the feed.

The monomolecular mechanism consists in the formation of the *n*-pentyl cation from *n*-pentane catalyzed by the solid acid. As recalled in [26] pentyl cation can be formed via three different routes (i) hydride abstraction on Lewis acid sites, (ii) protonation of pentane followed by H_2 removal, and (iii) protonation of pentene formed through dehydrogenation of pentane. The rearrangement of the pentyl cation into methyl-substituted cyclopropyl cation followed by ring opening and hydrid transfer leads to the desorption of isopentane,

$$C_5H_{12} \rightarrow C_5H_{11}^+ \rightleftharpoons C\text{–}\overset{\overset{C}{/\ \backslash}}{C^+\!\!-\!\!C}\text{–}C \rightarrow iC_5H_{11}^+ \overset{+H^-}{\rightarrow} iC_5H_{12}. \quad (1)$$

A bimolecular mechanism proceeds via dimeric C_{10}^+ species, formed from the reaction of C_5^+ or $C_5^=$ alkene. $C_5^=$ alkene may either be present in the feed as impurity or most probably formed due to the inevitable equilibrium of the pentyl cations with their deprotonation molecules

$$(CH_3)_2\text{–}C^+\text{–}CH_2\text{–}CH_3 \rightleftharpoons (CH_3)_2C{=}CH\text{–}CH_3 + H^+. \quad (2)$$

Dimeric C_{10}^+ species rearrange according to the fast alkyl cation transformations and experience very fast β-scission of the tertiary alkyl cation.

The bimolecular mechanism thus includes first pentyl cation formation–dimerization–β-scission–final hydrid transfer steps. The reaction products from *n*-pentane will include isopentane, propane, butanes, and hexanes. Consequently the monomolecular isomerization mechanism of pentane involves only *sec*- and *tert*-pentyl cations which cannot undergo facile β-cleavage. The cracking reaction $C_5 \rightarrow C_3 + C_2$ does not play a significant role; monomolecular mechanism leads to high selectivity into isopentane. By contrast, the bimolecular mechanism, where multibranched C_{10}^+ are formed, undergoes facile β-cleavage. With iC_5, large quantities of C_3 to C_5 fragments are formed resulting in a low selectivity to isopentane. According to this, two possible mechanisms for the reaction of *n*-pentane, intermolecular and intramolecular pathways, the results obtained in the present work are rationalized in the following.

Over bare HPA or SO_4–ZrO_2 assumed to be strong acids, C_5H_{12} activation by the catalyst at 423 K apparently occurs with the subsequent formation of $C_5H_{11}^+$ cations. From the present study it is not possible to discriminate whether the formation of pentyl cation involves hydrid abstraction on Lewis acid sites or pentane protonation on Brønsted acid sites. Recently is was concluded [27] that although pentyl cation may form either on Lewis acid sites or on Brønsted acid sites, pentyl cation generates surface pentene only on Brønsted acid sites. Over Lewis acid sites, the formation of surface pentene is inhibited because the pentyl cation is stabilized by interaction of lattice oxygen. The authors concluded that the monomolecular mechanism occurs on a Lewis acid site while the bimolecular mechanism involves the Brønsted acid site. In superacid media such as HF-SbF_5, the strength of the Brønsted acidity is very high such that the pentyl cation formed could hardly be deprotonated into pentene. The protonation–deprotonation equilibrium in superacid medium is shifted toward the protonated form

$$C_5H_{11}^+ \rightleftharpoons C_5H_{10} + H^+. \quad (3)$$

If the acid strength of HPA (or SO_4–ZrO_2) was as high as HF-SbF_5, the deprotonation equilibria of $C_5H_{11}^+$ cation would have been suppressed and pentene molecules would have not existed in the medium.

Only the monomolecular mechanism would have been operative. Tables 1–4 indicate that cracking of pentane has occurred to a large extent, and isobutane is the main reaction product. Thus these results provide unambiguous conclusion for a bimolecular mechanism in the reaction of *n*-pentane over bare HPA (or SO_4–ZrO_2). The reason for this is that pentyl cations are in equilibrium with their deprotonated pentene molecule. It is concluded that the acidity of these solid acids, in contrast with liquid superacids, cannot stabilize the protonated form. The catalytic behavior in *n*-pentane reactions would categorize HPA and SO_4–ZrO_2 not as superacids but rather as strong solid acids in agreement with previous investigations [28]. Bare HPA (and SO_4–ZrO_2) deactivate rapidly with time on stream as shown in Figs. 2 and 4. The deactivation occurred similarly at 423 or 473 K irrespective of the presence of H_2. The cause of deactivation is probably due to the formation of allylic and polyenylic residues, possibly of cyclic structure [25] which poison the acid sites of the catalyst. Such cations with polymeric structure have been identified in the polymerization of olefins in concentrated sulfuric acid [29,30]. This assumption of deactivation by acid site poisoning is supported by the appearance on the IR spectra of the used catalysts, of bands at 2927 and 2854 cm^{-1}, ascribed to $\nu_{C\text{–}H}$ vibrations of carboneous residue. From the results shown in Tables 1–4, one could not exclude that isopentane was also formed via a monomolecular path. Over bare HPA the selectivity to isobutane decreased as the conversion of n-C_5 decreased with time on stream at 423 and 473 K as well with or without H_2 in the feed. Simultaneously, the selectivity to isopentane increased. One can assume that the concentrations of $C_5H_{11}^+$ cations and C_5H_{10} molecules adsorbed on the surface decreased with the catalyst deactivation. Oligomerization, as a bimolecular reaction, depending on the concentration of both the carbenium ions and the alkene, will decrease more than the monomolecular rearrangement of $C_5H_{11}^+$. The results presented in Tables 1 and 3 indicate, as already stated, that H_2 has no effect on the overall activity and stability nor on the product distribution. Therefore one could suggest that

over bare HPA or bare SO_4–ZrO_2 no activation of molecular hydrogen occurred. The absence of *n*-pentane conversion at temperature less than 473 K over bare H-mordenite reflects the very high activation energy for protonation of pentane over H-mordenite and confirms the lower acid strength of zeolites as compared with HPA or SO_4–ZrO_2.

As to the reaction of *n*-pentane over Pt-containing solid acid catalysts, Fig. 2b and Table 2 indicate that the addition of platinum to HPA catalyst has no effect on the conversion of pentane with time on stream if the reaction was carried out at 423 K in the absence of H_2. The product distribution is not modified. These results indicate that under these conditions over both HPA and Pt-HPA catalysts the reaction mechanism was bimolecular and monofunctional. It is concluded that the metallic function of Pt-HPA was not efficient enough to dehydrogenate pentane, at a reasonable rate at 423 K. Consequently, the concentration of pentene from dehydrogenation on platinum was very low and hence no bifunctional character of the reaction appeared. The striking effect of platinum appeared when the conversion of pentane was carried out in the presence of H_2. At 423 K, in the presence of platinum, H_2 suppressed the *n*-C_5 reaction. As stated above, it has been proposed that over Pt-HPA, the reaction mechanism at 423 K was monofunctional and bimolecular. In H_2, over Pt-HPA, the olefinic species, such as C_5H_{10}, responsible for the bimolecular path is hydrogenated into C_5H_{12} [Eq. (4)] at a rate faster than that of dimerization reaction to form $C_{10}H_{21}$ cation [Eq. (5)]:

$$\text{hydrogenation:}\quad {C_5H_{11}}^+ \overset{-H^+}{\rightleftharpoons} C_5H_{10} \xrightarrow[H_2]{Pt} C_5H_{12}, \tag{4}$$

$$\text{dimerization:}\quad {C_5H_{11}}^+ + C_5H_{10} \rightleftharpoons {C_{10}H_{21}}^+. \tag{5}$$

The surface concentration of olefin intermediates which are in equilibrium with ${C_5H_{11}}^+$ would be very low. The result is that the bimolecular mechanism would be suppressed over Pt-HPA catalyst when H_2 was cofed. If dehydrogenation of pentane over platinum occurs at a too low rate the bifunctional mechanism for *n*-pentane isomerization also could not operate. Interestingly, from the results obtained for the reaction of *n*-pentane at 473 K in H_2 over Pt-HPA, Fig. 2a and Table 1, two noteworthy observations can be made: selectivity toward isopentane is near 100%, indicating that a monomolecular mechanism is operating and conversion with time on stream is constant, indicating that the surface polyolefinic intermediates do not accumulate on the acid sites. Thus one could suggest that, at 473 K in H_2, dehydrogenation of pentane into pentene over platinum would occur to provide enough C_5H_{10} concentration to initiate the monomolecular carbenium ion mechanism. Thus the pool of C_5H_{10} at higher temperature is no more provided via deprotonation of the pentyl cation [Eq. (3)] but via *n*-pentane dehydrogenation on platinum

$$C_5H_{12} \rightleftharpoons C_5H_{10} + H_2. \tag{6}$$

At 473 K, although the equilibrium concentration of pentene is decreased in the presence of hydrogen, thus lowering the reaction rate for pentane isomerization, the forming polyolefinic residues may be promptly hydrogenated thus favoring their desorption from the solid acid surface. Catalyst deactivation is hence prevented.

The conversion of *n*-pentane also decreased rapidly with time on stream in the presence of *Pt-free SO_4–ZrO_2* (Fig. 4). The deactivation behavior of sulfated zirconia occurred with or without H_2 in the feed. As is shown in Tables 3 and 4 *n*-pentane is mostly undergoing a cracking reaction, predominantly into isobutane. The product distribution indicates that the reaction proceeds via a bimolecular mechanism at both 423 and 473 K. Similarly to HPA, sulfated zirconia initiates the activation of pentane at as low temperature as 423 K via processes in which ${C_5H_{11}}^+$ and ${C_{10}H_{21}}^+$ species are formed. Subsequent multibranching isomerization, β-scission, and hydride transfer finally produce mainly isobutane and isopentane. Interestingly it is found (Table 3), in contrast to HPA, that at 423 K, the product distribution did not change significantly with time on stream; isobutane being predominantly formed even at low conversion over the deactivated samples. Based on the above discussion one could suggest that the acid strengths of HPA and SO_4–ZrO_2 samples investigated in this work were very similar, favoring the bimolecular mechanism in the reaction of *n*-pentane. The bimolecular mechanism prevailed for the reaction of *n*-pentane over Pt-containing SO_4–ZrO_2 at 473 K in the absence of H_2. Catalyst deactivation due to coking and preferential formation of isobutane and isopentane, reported in Fig. 4 and Tables 3 and 4 support this conclusion. In the presence of H_2, the bimolecular path, in the isomerization of *n*-C_5 at 423 K over Pt-containing SO_4–ZrO_2, is suppressed as indicated by the zero conversion of *n*-C_5. The suppression of the *n*-C_5 reaction at 423 K may be explained by the insufficient acid strength of SO_4–ZrO_2 to isomerise ${C_5H_{11}}^+$ cations via a monomolecular path at an appreciable rate, while the pentene issued from the reaction is instantaneously hydrogenated by H_2 in the presence of platinum [Eq. (4)].

One could suggest that the rate of pentene hydrogenation is much faster than the rate of C_5H_{10} addition to ${C_5H_{11}}^+$ [Eq. (5)]. Therefore the bimolecular mechanism would be almost suppressed over Pt–SO_4–ZrO_2 catalysts when H_2 is present.

Like the behavior of Pt-HPA catalysts, at 473 K in H_2, over Pt–SO_4–ZrO_2, the dehydrogenation equilibrium of pentane into pentene [Eq. (6)] is fast enough and substantially shifted so that a reasonable concentration of C_5H_{10} olefin is achieved. Therefore a bifunctional monomolecular mechanism accounts for the isomerization of *n*-pentane in H_2 at 473 K over Pt–SO_4–ZrO_2.

In earlier studies involving the reaction of *n*-pentane over H-mordenite and over Pt–H-mordenite [3] it was found that platinum favors the formation of isopentane and also enhances the stability with time on stream. The same trend is observed in the present work. For *bare H-mordenite* when the reaction of pentane was carried out with or without H_2

in the feed fast deactivation occurred (Fig. 5). Table 5 also indicates that the selectivity to isopentane is low. This behavior is the result of the monofunctional bimolecular character of the reaction over bare H-mordenite. $C_5H_{11}^+$ ions generated over the acid sites of H-mordenite in equilibrium with C_5 olefins in the pores experience a typical bimolecular condensation reaction for the generation of $C_{10}H_{21}^+$ carbenium ions followed by skeletal isomerizations and finally cracking which generates isobutane, *n*-butane, isopentane, and propane. Regarding the selectivities of the products, it is observed that large amounts of *n*-butane and propane were produced over H-mordenite in comparison with HPA or SO_4–ZrO_2. The fact that the selectivity for *n*-butane, or the molar ratio n-C_4/iC_4, is higher over H-mordenite indicates that the cracking product intermediates were less branched within H-mordenite. This is because the constraint exerted by the small size of the H-mordenite pores limits the formation of highly multibranched C_{10}^+ intermediates. It is well known that the molar ratios n-C_4/iC_4 in the cracking product distribution decreases with increasing the branching of the intermediate carbenium ions. To justify the absence of the *n*-pentane reaction at 423 K over H-mordenite as compared with HPA or SO_4–ZrO_2 we have proposed that the acid sites of H-mordenite are of lower strength. The higher molar ratio n-C_4/iC_4 over H-mordenite is also probably due to the same reason. Indeed, multibranching of C_{10}^+ intermediates depend on their average life time which is relatively low when the strength of the acid sites is low. The lower acid strength of H-mordenite compared to HPA or SO_4–ZrO_2 results in the shifting of a cracked product spectrum from isobutane to more *n*-butane and propane. The absence of any effect of H_2 on the catalytic behavior of *Pt-free H-mordenite* in the *n*-pentane reaction is consistent with a monofunctional acid mechanism.

In the reaction of *n*-pentane at 498 K over the hybrid Pt–SiO_2/H-mordenite catalyst, H_2 affected considerably the conversion and its change with time on stream (Fig. 5a) and the product distributions (Table 5). At 498 K the hybrid catalyst Pt-HM behaves more or less like a true bifunctional catalyst. According to the classical bifunctional mechanism, pentane is dehydrogenated into pentene on the platinum sites and pentene formed is protonated on the acid sites yielding pentyl cations. Isomerization to isopentane would then result from intramolecular rearrangement of the *sec*-pentyl cations (monomolecular path) or from dimerization-cracking reactions (bimolecular path). The results in Table 5 allow discrimination among the monomolecular and bimolecular mechanisms. In the absence of H_2 the selectivity into isopentane is low and large amounts of propane, isobutane, and *n*-butane are formed. Thus in the absence of H_2 the bimolecular mechanism prevailed on Pt-HM. The bimolecular mechanism apparently is suppressed by adding H_2 in the feed (Table 5). This table indeed indicates that in H_2 the selectivity to isopentane was as high as 84%, with negligible amounts of C_3 and C_4 detected. This bimolecular reaction path depends, like the oligomerization reaction, on the concentrations of pentyl cations and of C_5 olefins. Considering that the thermodynamic dehydrogenation equilibrium of pentane into pentene [Eq. (6)] has been reached, the presence of H_2 in the feed decreases the nominal concentration of pentene. As a consequence the reaction rate of the bimolecular path would decrease more than that of monomolecular path. In addition the overall reaction rate of pentane over bifunctional Pt-HM, which depends on the equilibrium concentration of the pentene formed on the platinum, will decrease by decreasing pentene concentration, thus by adding H_2 in the feed in agreement with the results shown in Table 5. The relative contribution of the bimolecular mechanism over H-mordenite-based catalysts is, as expected, dependent on reaction conditions as temperature, feed composition, and conversion level and on the catalyst composition as well.

5. Conclusion

The reaction of *n*-pentane over solid acid catalysts occurs through two parallel paths: an intermolecular oligomerization-cracking process which results in relatively low isopentane selectivity and an intramolecular skeletal rearrangement process where the selectivity in isopentane is high. Over bare heteropolyacids, SO_4–ZrO_2 and probably WO_x–ZrO_2, the bimolecular mechanism is favored, particularly at the lowest reaction temperatures. The production of isopentane is accompanied with cracked products, propane, and butanes. The acid strength of these solids is not high enough to prevent the deprotonation of $C_5H_{11}^+$. Consequently dimerization-cracking reactions become inevitable. It has been shown that carbon monoxide suppresses the process of conjunct polymerization as the result of the carbonylation of $C_5H_{11}^+$ or/and C_5H_{11} (3). By contrast, chlorinated alumina behaves more like a superacid, since apparently the deprotonation equilibrium

$$C_5H_{11}^+ \rightleftharpoons C_5H_{10} + H^+ \tag{3}$$

is suppressed and consequently isomerization of pentane is intramolecular leading to high selectivity. Over hybrid Pt-HPA, Pt–SO_4–ZrO_2 catalysts, the bifunctional mechanism for pentane reactions appears at relatively high temperatures due to the low value of the thermodynamic dehydrogenation constant. At high temperatures, the presence of H_2 in the feed suppresses the bimolecular mechanism due to fast hydrogenation of the olefins, $C_5H_{11}^+$ cations experiencing only the intramolecular rearrangement into *tert*-pentyl cations. At lower reaction temperatures, where the concentration of C_5H_{10} from dehydrogenation on platinum is very low, the reaction occurs via a monofunctional bimolecular mechanism only. H_2 suppresses the reaction over Pt-HPA and Pt–SO_4–ZrO_2. Finally due to its lower acid strength, monofunctional H-mordenite as well as bifunctional Pt-H-mordenite requires higher reaction temperatures than HPA

or SO_4–ZrO_2, high isopentane selectivity being reached only over Pt-containing mordenite in the presence of H_2 in the feed.

References

[1] G. Bour, C.P. Schwoerer, G.F. Asselin, Oil Gas J. 68 (1970) 43.
[2] K.J. Ware, A.H. Richardson, Hydrocarbon Process. 51 (1972) 11.
[3] H.W. Kouwenhoven, Molecular Sieves, in: ACS Advances in Chemistry Series, Vol. 121, Am. Chem. Society, Washington, 1973, p. 529.
[4] P.B. Koriada, J.R. Kiosky, M.Y. Asim, J. Catal. 66 (1980) 290.
[5] J.A. Gray, J.T. Cobb, J. Catal. 36 (1975) 125.
[6] A. Hollo, J. Hancsok, D. Kallo, Appl. Catal. A 229 (2002) 93.
[7] Y. Liu, G. Koyano, M. Misono, Top. Catal. 11/12 (2000) 239.
[8] Y. Liu, G. Koyano, M. Misono, Top. Catal. 11/12 (2000) 239.
[9] N. Essayem, Y. Ben Tâarit, P.Y. Gayraud, G. Sapaly, C. Naccache, J. Catal. 203 (2001) 157.
[10] B.B. Bardin, R.J. Davis, Top. Catal. 6 (1998) 77.
[11] X. Song, A. Sayari, Catal. Rev. Sci. Eng. 38 (1996) 329.
[12] G.D. Yadav, J.J. Nair, Micropor. Mesopor. Mater. 33 (1999) 48.
[13] V. Adeeva, H.Y. Liu, B.Q. Xu, W.H.M. Sachtler, Top. Catal. 6 (1998) 61.
[14] S. Rezgui, R.E. Jentoft, B.C. Gates, Catal. Lett. 51 (1998) 229.
[15] S.Y. Kim, J.G. Goodwin, S. Hammache, A. Auroux, D. Galloway, J. Catal. 201 (2001) 1.
[16] G. Barton, S.L. Soled, G.D. Meitzner, G.A. Fuentes, E. Iglesia, J. Catal. 181 (1990) 57.
[17] S.V. Filimonova, A.V. Nosov, M. Scheithauer, H. Knözinger, J. Catal. 198 (2001) 89.
[18] J.G. Santiesteban, D.C. Calabo, C.D. Chang, J.C. Vartuli, T.J. Fiebig, R.D. Bastian, J. Catal. 202 (2001) 25.
[19] P.Y. Gayraud, N. Essayem, J.C. Vedrine, Stud. Surf. Sci. Catal. 130 (2000) 2549.
[20] N. Essayem, R. Frety, G. Coudurier, J.C. Védrine, J. Chem. Soc., Faraday Trans. 93 (1997) 3243.
[21] A. Patel, G. Coudurier, N. Essayem, J.C. Vedrine, J. Chem. Soc., Faraday Trans. 93 (1997) 347.
[22] A. Auroux, in: Proceedings of the 29th North American Thermal Analysis Society Conference, St. Louis, MO (September 24–26, 2001), 2001.
[23] T. Okuhara, T. Nishimura, M. Misono, Stud. Surf. Sci. Catal. 101 (1996) 559.
[24] H. Liu, G.D. Lei, W.M.H. Sachtler, Appl. Catal. A 137 (1996) 167.
[25] M.V. Luzgin, A.G. Stepanov, V.P. Shmachkova, N.S. Kotsarenka, J. Catal. 203 (2001) 273.
[26] Y. Liu, K. Na, M. Misono, J. Mol. Catal. A 141 (1999) 145.
[27] H. Matsuhashi, H. Shibata, H. Nakama, K. Harata, Appl. Catal. A 187 (1999) 99.
[28] N. Essayem, G. Coudurier, J.C. Védrine, D. Habermacher, J. Sommer, J. Catal. 183 (1999) 292.
[29] V.N. Ipatief, H. Pines, J. Org. Chem. 1 (1936) 464.
[30] H. Pines, The Chemistry of Catalytic Hydrocarbon Conversion, Academic Press, New York, 1981.